ACS MEASUREMENT SCIENCE Au
AN OPEN ACCESS JOURNAL OF THE AMERICAN CHEMICAL SOCIETY

pubs.acs.org/measureau
Article

E.Co.Tech Breathalyzer: A Pilot Study of a Non-invasive COVID-19 Diagnostic Tool for Light and Non-smokers

Ivneet Banga,[§] Kordel France,[§] Anirban Paul, and Shalini Prasad*

Cite This: ACS Meas. Sci. Au 2024, 4, 496−503
Read Online

ABSTRACT: Analysis of exhaled breath offers a noninvasive approach to understanding the metabolic state of the body. This study focuses on the efficacy of an innovative Electrochemical Hand-held Breathalyzer COVID-19 Sensing Technology (E.Co.Tech) for predicting COVID-19 infection, specifically in populations of never or former light smokers. The electrochemical nose technology used in this device aims to discriminate changes in exhaled nitric oxide levels, which are associated with COVID-19-linked respiratory inflammation. The methodology combines the device with a machine learning-based algorithm trained on a diverse data set of breath profiles from both infected and noninfected individuals. A cohort of 46 participants, consisting of never or former light smokers, was recruited. Each participant was tested using the E.Co.Tech prototype device and an iHealth COVID-19 antigen rapid test. The performance of the device was assessed by calculating sensitivity, specificity, positive predictive value, and negative predictive value (NPV). The results demonstrated high specificity (91.11%) and NPV (97.62%) for the device in this demographic group. This case study underscores the potential of E.Co.Tech as a valuable tool for point-of-care COVID-19 diagnosis, particularly in populations with unique smoking histories. The technology's high sensitivity and specificity, along with its rapid results, make it a promising candidate for deployment in resource-limited settings and situations where timely detection is crucial for effective public health management. Further large-scale clinical trials and real-world validations are necessary to establish the device's utility across diverse population groups.

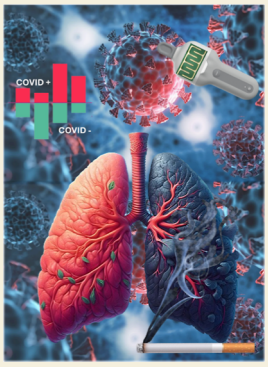

KEYWORDS: *COVID-19, electrochemistry, chronoamperometry, room temperature ionic liquid, breath analyzer, nitric oxide*

INTRODUCTION

The SARS-CoV-2 virus, commonly known as COVID-19, poses a worldwide threat, impacting millions of individuals and persisting as an ongoing concern. Its immediate effects have been evident over the past two years. Vaccination efforts have reached nearly 13 billion individuals worldwide in the fight against the pandemic.[1] Despite these measures, new cases continue to emerge due to the evolving nature of the virus through mutations. A lingering condition known as long COVID-19, or postacute sequelae of COVID-19, involves a range of severe symptoms that follow infection with the SARS-CoV-2 virus.[2]

Long COVID-19 affects individuals of all age groups and various levels of disease severity, with the highest diagnosis rates occurring between 36 and 50 years old. The majority of long COVID-19 cases are observed in patients who did not require hospitalization for their initial mild acute illness.[3] This is significant as these nonhospitalized cases constitute the majority of overall COVID-19 cases. Of the entire population impacted by COVID-19, approximately 20% have been hospitalized, underscoring the need to comprehend the long-term consequences for survivors.[4] Exposure to cigarette smoke accelerates the decline of forced expiratory volume in 1 s (FEV1), ultimately resulting in a blockage of airflow (FEV1/FVC < 0.7).[5] This obstruction in airflow and the subsequent reduction in flow rates can be attributed to structural abnormalities such as emphysema. These changes can occur independently or in combination with inflammatory cells and mucus, leading to the narrowing of small airways.[6,7] Even if individuals quit smoking, the accelerated rate of decline in lung function is not entirely reversible. This implies that individuals with even minimal smoking histories are at risk of developing symptomatic respiratory diseases in the long term. Impairment in the capacity for pulmonary diffusion may manifest before a reduction in FEV1 and is associated with more severe symptoms and reduced exercise tolerance. However, FEV1 remains the most commonly used physiological measurement for diagnosing and monitoring such diseases. Unfortunately, quantitative assessments of diseases affecting small airways and emphysema are not routinely performed.[8]

There is insufficient recognition of the need for a comprehensive evaluation of various physiological measurements beyond FEV1 when considering the impact of smoking

Received: April 17, 2024
Revised: July 3, 2024
Accepted: July 5, 2024
Published: July 25, 2024

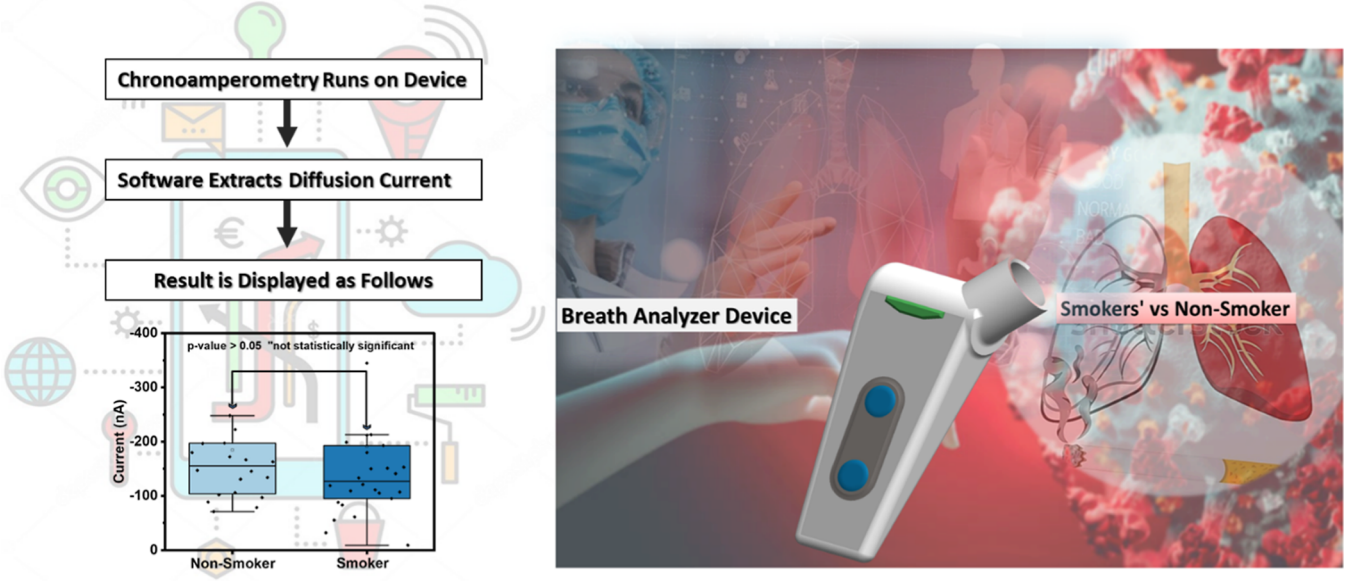

Figure 1. Schematic representation of the working scheme for the breath analyzer platform.

exposure. Inhaling cigarette smoke has been demonstrated to bring about immediate changes in the lungs, affecting factors such as airway resistance, coughing, and airway irritation.[9] This suggests that even in the early stages of smoking, there could be effects on respiratory function. In June 2020, the World Health Organization issued a report cautioning that smoking habits might have an unfavorable impact on the prognosis of COVID-19. Drawing from substantial evidence, the report emphasized the detrimental influence of tobacco use on lung health and its causal link to both viral and bacterial respiratory infections.[10] In humans, the interaction between the spike protein and angiotensin-converting enzyme 2 (ACE2) forms a binding site for the SARS-CoV-2 spike protein. Notably, ACE2 expression was found to be elevated in the small airway epithelia of smokers, partially accounting for the heightened risk of severe COVID-19 among this subgroup. However, studies conducted in various countries, both European and non-European, such as China, the United States, Mexico, Israel, France, the United Kingdom, and Italy, have revealed an unexpectedly low prevalence of active smokers among hospitalized COVID-19 patients when compared to the general population. Additionally, an ecological study involving 38 European countries and some nonhospitalized populations unveiled a negative correlation between the current prevalence of smoking and the occurrence of COVID-19 at the population level. Potential biological mechanisms have been suggested to explain this counterintuitive underrepresentation of smokers among COVID-19 patients, further highlighting the existence of the "smoker's paradox" phenomenon.[11,12]

Exhaled breath has emerged as a valuable tool for noninvasive disease diagnosis through a field of study commonly referred to as "breathomics".[13] Exhaled breath is composed of both a gaseous and a liquid phase. The gaseous phase contains elements like oxygen, nitrogen, carbon dioxide, nitric oxide (NO), and volatile organic compounds (VOCs) present in concentrations ranging from parts per million to parts per billion.[14] These VOCs originate from cellular metabolic activities within the body.[15] Within exhaled breath, there exist thousands of VOCs that offer insights into various diseases, including lung cancer, chronic kidney disease, asthma, chronic obstructive pulmonary disease, and even the highly lethal SARS-CoV-2 virus[16,17,18−20] The field of metabolomics, often referred to as breathomics, holds substantial potential for providing noninvasive diagnostic tools for a range of diseases. Violi et al. conducted a study that supported the hypothesis of NOX2 overactivation in COVID-19 patients, showing a more than 40% increase compared to control subjects.[21] The research indicates that COVID-19 patients, especially those admitted to the intensive care unit, display heightened NOX2 activation compared to control subjects. Another study confirmed that the activation of NOX genes is heightened by the release of NO from human endothelial cells.[22] Currently, there is only one breath analyzer: FeNO by NIOX, available in the market, which detects fractional NO using electrochemical method.[23] Aside from this, there are only few prototypes reported in literature suggests the detection of NO.[24−26] These products are observed to have several other issues including high cost and sophisticated, restricted field use. Advancements in analytical platforms have facilitated the increased use of VOCs as markers to indicate disease exposure. This has consequently raised the potential for developing noninvasive biomarker-based breath profiling techniques for both acute and chronic disease detection. Researchers are actively engaged in creating markers that can aid in the early detection of diseases, thereby contributing to timely intervention and treatment.[27,28]

This work focuses on expanding point-of-care diagnostics via breathomics. Here, we build off of an innovative Electrochemical Breathomics Sensing Technology[29] (E.Co.Tech) for its efficacy in predicting COVID-19 infection in this specific demographic group. With the work of E.Co.Tech, they define a point-of-care breathalyzer that leverages electrochemical principles to detect NO in exhaled breath samples, a characteristic signature associated with various viral infections including COVID-19. The methodology employed in this research combines the device with a machine learning-based algorithm trained on a diverse data set of breath profiles from both infected and noninfected individuals. We advance the work of E.Co.Tech by showing how a similar technology can be designed such that its performance is not dissuaded by compounds present in patients who have a large smoking

https://doi.org/10.1021/acsmeasuresciau.4c00020
ACS Meas. Sci. Au 2024, 4, 496−503

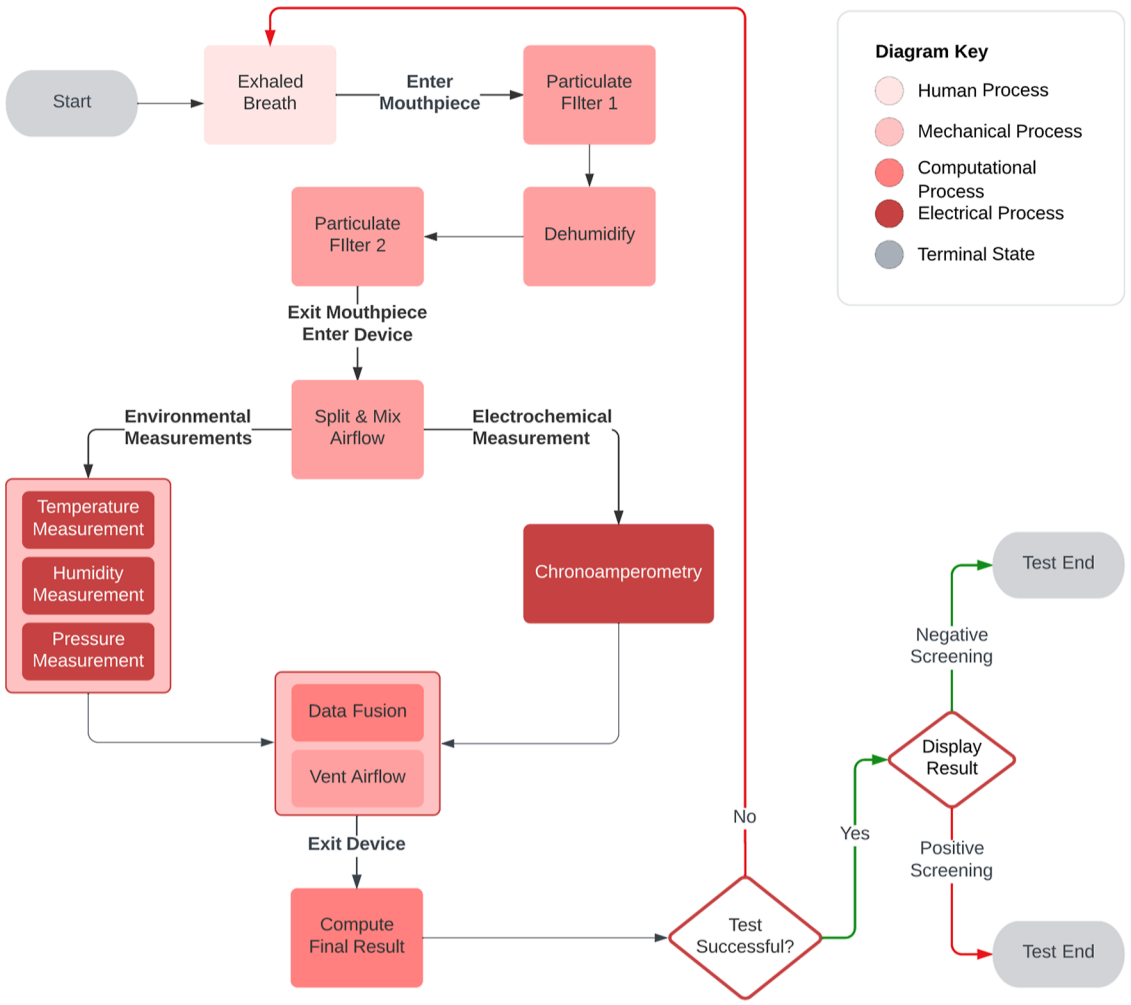

Figure 2. Diagram of the test procedure is shown above, indicating how electrochemical and computational processes occur throughout to obtain a result for each subject.

history. We hypothesize that a device based on the E.Co.Tech technology is robust enough to accurately detect high levels of NO even when confounding factors are present, such as those found in the breath of heavy smokers. As a result, a cohort of 46 patients containing both nonsmokers and former light smokers was recruited. Participants were tested using both the E.Co.Tech based prototype device and an iHealth COVID-19 antigen rapid test. The ensuing data sets were rigorously subjected to statistical analysis, with the latter acting as the control. Sensitivity, specificity, positive predictive value, and negative predictive value (NPV) were calculated to assess the performance of the device. Results demonstrate a high correlation between the device response and the underlying condition. This case study underscores the potential and robustness of the device as a valuable tool in the point-of-care diagnosis of COVID-19, particularly in demonstrating the ability to nullify smoking as a convoluting factor in electrochemical signals.

RESULTS AND DISCUSSION

A use case scenario is illustrated as a schematic diagram in Figure 1. To evaluate our hypotheses, we developed a portable NO sensing prototype device in the form of a breath analyzer. The device contains an electrochemical sensor and two microcontrollers that work collaboratively—one acting as a primary controller to coordinate driver functions of the device and the other as a secondary controller over a potentiostat that performs analysis on stimuli received by the electrochemical sensor. In this work, those stimuli are VOCs (Figure 1). The electrochemical sensor contains an interdigitated electrode (IDE) spin-coated with room temperature ionic liquid (RTIL) measuring EMIM[BF4] as the target analyte. We document our electrochemical response in nanoamperes (nA) but perform measurement resolution in picoamperes (pA). A picoampere is an extremely small magnitude in electrical current. Those familiar with electrical design may observe that this finite of a measurement could potentially be mistaken as electromagnetic noise. Solving this came down to careful electrical engineering. With the device we present here, we have taken the necessary engineering discipline to electromagnetically shield our sensors, potentiostat, and overall electronic design to ensure that the signal we do measure cannot be mistaken as noise. A user's breath is transferred to the sensor through a single-use disposable mouthpiece that is inserted at the top of the breath analyzer. In many electrochemical analyses, excess water can severely convolute the signal. As a result, the mouthpiece contains desiccant for the removal of humidity and multiple dual-layer synthetic fiber filters for filtration of the air as it enters the analysis chamber of the device. The comprehensive test procedure outlined below

https://doi.org/10.1021/acsmeasuresciau.4c00020
ACS Meas. Sci. Au 2024, 4, 496−503

(Figure 2) illustrates the seamless integration of electrochemical and computational processes at every stage, culminating in the acquisition of results for each subject. From meticulous sample preparation and rigorous electrochemical testing to the sophisticated application of computational modeling, this methodology synergistically combines experimental data with predictive simulations.

The detailed testing procedure is outlined as follows. The user initiates a breath test by pressing a button on the device. Following this initiation, the device instructs the user to wait as it assesses baseline values for the target analyte in the current ambient environment. This assessment is conducted through a chronoamperometric sequence managed by the potentiostat, referred to as the "baseline sequence", with the results stored locally for future reference. Once the baseline sequence concludes, the user is prompted to exhale into the device through the mouthpiece. Simultaneously, the device begins an identical chronoamperometry sequence, known as the "stimulus sequence". This sequence evaluates the values of the target analyte as the patient breathes. The only difference between the baseline and stimulus sequences is that the latter occurs as breath passes over the sensor, while the former is only measuring ambient air. Although a six-second breathing window is allocated for the stimulus sequence, a mere 3 s are required to obtain a sufficient result.

Following the stimulus sequence, embedded algorithms within the device extract the 6 s diffusion current value and compare it to the results obtained from the baseline sequence. The difference between the baseline and stimulus sequence is then saved and categorized as either positive (indicating strong evidence of NO detection) or negative (suggesting insufficient evidence of NO to be considered significant). At this stage, the assessment is deemed complete, with an optional step allowing for the wireless transmission of assessment results to a database for storage or to a mobile application for convenient visualization.

During both the baseline and stimulus sequences, several other sensors perform local measurements of the environment around the sensor IDE. Namely, these additional sensors assess temperature, pressure, and humidity of both the ambient environment and the observed breath. Environmental factors can heavily bias the response of the final test readings as the RTIL-based electrochemical sensors are most accurate within specific temperature, humidity, and flow pressure windows. Therefore, the electrochemical response must be corrected to compensate for this bias. To do so, we leverage the following equations for temperature and relative humidity

$$x_{\text{temp\_c}} = (0.148082 \times x_{\text{raw}}) + 25.478439\, e^{(2.694800\, e^{-9} k_{\text{rh}})} - 25.478439 \quad (1)$$

$$x_{\text{rh\_c}} = (0.148082 \times x_{\text{temp\_c}}) - 0.999258\, e^{(-2.233200\, e^{-9} k_{\text{temp}})} + 0.999258 \quad (2)$$

where x_{raw} denotes the raw electrochemical signal of the breath uncorrected for any variables, k_{rh} denotes the relative humidity of the breath prior to correction, k_{temp} denotes the temperature of the breath prior to correction, $x_{\text{temp\_c}}$ defines the electrochemical signal after temperature correction, and $x_{\text{rh\_c}}$ defines the electrochemical signal after relative humidity correction. These equations are experimentally derived using regression techniques over a battery of tests performed in the laboratory under stepped pressure, temperature, and humidity levels. The raw electrochemical signal is first corrected for temperature in eq 1 and then that result is used as input to eq 2 to correct for relative humidity. Examples of regression fits to these equations can be found in the Supporting Information (Figures S3 and S4). Pressure had much less influence on the electrochemical signal and therefore did not require a correction equation. While these equations help us establish a common frame of reference, our test data aligns with other literature in supporting that electrochemical response from environmental fluctuations are inherently nonlinear, and that the above correction equations may not apply if outlying environmental conditions are encountered.[30,31] Therefore, we designed the mouthpiece to instantiate a series of experimental controls to ensure we captured consistent and reliable data throughout our study.

Desiccant acts as a normalizing mechanism for pressure, humidity, and temperature. Humidity is removed from the breath as it passes through the desiccant. For the results in these experiments, we selected the sSORB AW13B white silica gel beads from Interra Global. As a reaction from the humidity extraction, the desiccant heats up. The desiccant bead size was carefully selected to ensure consistency in airflow turbulence as the breath passes through the mouthpiece, which regulates pressure as a result. Experimental results showed desiccant bead sizes of 1−3 mm gave optimal throughput of airflow while slowing the air down enough to a narrow enough pressure window. The mass of desiccant was also optimized to 320 g to ensure that, upon exit of the mouthpiece, the breath's relative humidity was between 10 and 20%, its temperature fell between 32 and 38 °C, and its exit pressure fell within a 6−7 mPA regardless of the breath's input condition. As a final form of control, the analysis chamber was constructed to ensure airflow hit the sensor at an angle between 12 and 20°. While at complete rest, the average adult male undergoes an exchange of approximately 0.5 L (500, 400 mL for females) of air per breath, known as tidal volume. This exchange occurs at a frequency of 12 breaths per minute, leading to a minute ventilation rate of approximately 6 L of air per minute.[32]

Even after correction, the chronoamperometric signals for each patient are very noisy. Filtering techniques like Kalman filters, exponential regression, and inverse regression were applied to each sample automatically by the software after acquisition to normalize the signal. In addition, thresholds for COVID-19 positive and negative signals needed to be established in order to determine how to classify each patient. To establish these thresholds, a machine learning algorithm called *K*-means clustering was leveraged over data acquired in the laboratory. A benchtop testing apparatus linked to NO and compressed try air lines at the university laboratory enabled us to acquire several hundred synthetic breath samples that allowed us to establish a data set of 300 in size. This data set was then used to train the clustering algorithm to cluster each data point into one of three groups: evidence of COVID-19 (positive), not enough evidence of COVID-19 found (negative), or not enough information to make a conclusion (unknown). These thresholds are 23 dimensions in size so this clustering occurs in high-dimensional space. The 23 dimensions for each sample size include 12 regression parameters; 2 parameters each for pressure, temperature, and humidity; 1 time parameter; and 4 electrochemistry parameters. Note that none of these parameters are specific to smokers which highlights the invariance of our statistical

https://doi.org/10.1021/acsmeasuresciau.4c00020
ACS Meas. Sci. Au 2024, 4, 496−503

methodology to smoker data. The high-dimensional clusters enable a single 1-dimensional scaler to be returned as an answer of either "positive" or "negative". It should be noted that, although "unknown" was a possible clustering label in our methodology above, we received tests that fell into this cluster neither during our benchtop analysis nor during human subject testing.

The data obtained for the breath sample collected from 46 human subjects can be seen in Figure 3. The *x*-axis represents the total number of subjects and the *y*-axis represents the final corrected changed in current between the baseline and stimulus sequences. We emphasize that the *y*-axis is the corrected change in current because the change in the current itself does not present enough information to facilitate an accurate indication of the respiratory condition; it must be weighted according to environmental factors discussed above and the rate of diffusion.

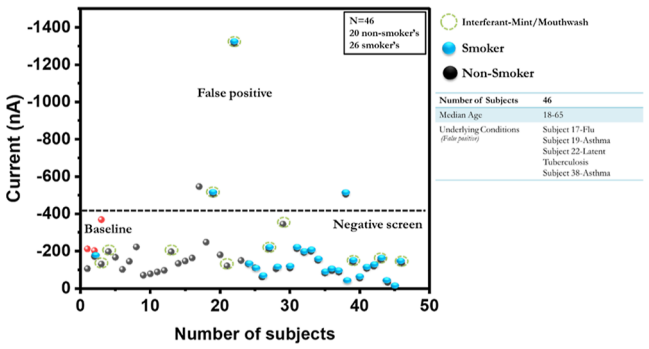

Figure 3. Sensor output indicating the change in electrical current as recorded by the breath analyzer device for 46 subjects. The response is plotted as a ratio metric signal wherein the signal is compared to the baseline.

A positive change between the baseline and stimulus sequences provides strong evidence to support a COVID-19 positive subject while a negative ratio provides strong evidence to support the absence of the disease. A positive signal is the current value is greater than the threshold value set, therefore has a positive change in current. However, in our study, we received 4 false positive as the subjects were tested using the iHealth rapid test. These results can be correlated to the presence of underling respiratory condition which can lead to the release of higher levels of NO in breath. Conversely, a negative change between the baseline and stimulus sequences that the total response is below the threshold set for the sensing NO.

In this study, 46 human subjects were tested: 19 nonsmokers and 27 smokers. The signal obtained is first depicted as a raw current value normalized against humidity, temperature, and pressure of the exhaled breath. This normalization provides for a common frame of reference to compare each test against. This proportion is more succinctly demonstrated by Figure S1, indicating the maximum absolute value of the measured current (nA) obtained during the breathing cycle for each subject. From these plots, one can see that the statistical difference between smokers and nonsmokers is not significantly different ($p > 0.05$).

Furthermore, we conducted principal component analysis (PCA) over 46 subjects to better assess the results. As mentioned above, each sample is 23 dimensions in size; humans cannot easily visualize greater than 3 dimensions. PCA is a dimensionality reduction technique commonly used within statistics and machine learning for visualizing multidimensional data sets.[33,34] Depending on the field of use, it is also known as singular value decomposition and the discrete Karhunen–Loève transform.[35] Other dimensionality reduction techniques such as *t*-distributed stochastic neighbor embedding (*t*SNE) was also investigated. However, *t*SNE attempts to preserve local relationships among data set features as a function of their distance in embedding space while PCA emphasizes the preservation of global structure as a function of covariances between features.[36] For this application, there is a need to ensure that global consensus across all data points is maintained, which is why PCA takes preference here. *t*SNE also requires training and hyperparameter tuning that may not generalize well in all scenarios. The test for each subject is

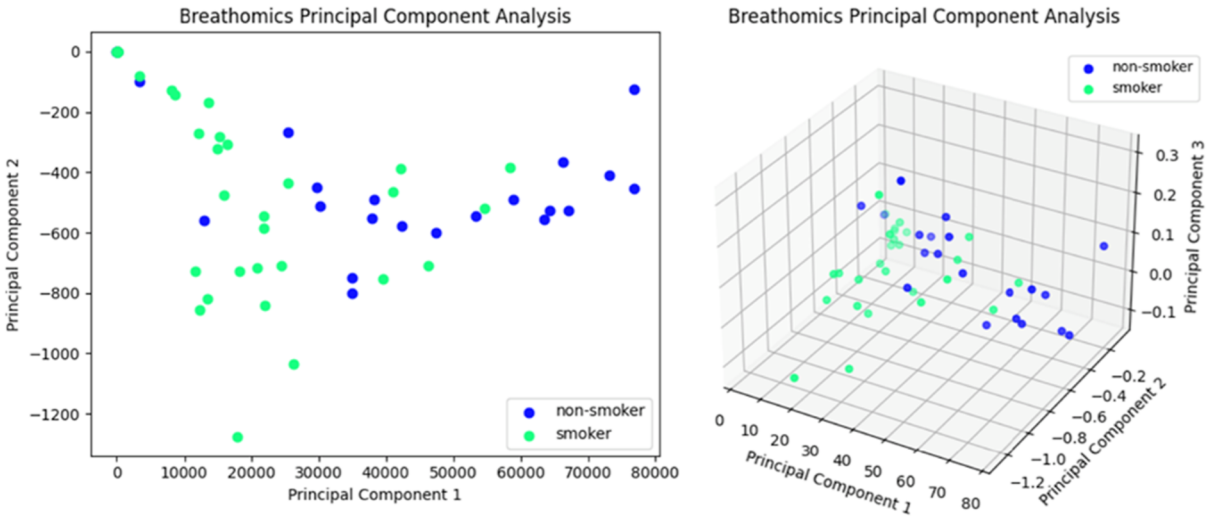

Figure 4. Dimensionality reduction to two and three dimensions performed via PCA is shown here. PCA works by breaking down the highest contributing components to the variance within the data, so the top 2 and 3 contributors (out of the full 23 parameters) to variance are shown here. They are dimensionless parameters. We note that, while there is no statistical difference between the results of smokers and nonsmokers for this study, their PCA results show that breath responses between the two categories are subtly different.

https://doi.org/10.1021/acsmeasuresciau.4c00020
ACS Meas. Sci. Au 2024, 4, 496−503

saved as a 23-dimensional vector, so dimensionality reduction through PCA significantly helps in the interpretation of statistical significance between the smoker and nonsmoker tests. Figure 4 shows these PCA results for both two and three dimensions. With all dimensionality reduction techniques, we seek to gain interpretation at the cost of some information loss from compressing dimensions. We can see this method in effect as we transition from two-to three-dimensional PCA in Figure 4. We see general uniform randomness between data points presented by the PCA plots in Figure 4. This is desired with PCA because it indicates that breath responses between smokers and nonsmokers are uncorrelated, providing more evidence to support our hypothesis that a patient's pulmonary history does not induce significant bias on our device's performance. However, in the transition from two dimensions to three dimensions, one may notice that smokers and nonsmokers seem to become easily separable. As we scale higher, we approach the true dimensionality with which each patient test was measured so we gain additional information.

While the final results between smokers and nonsmokers showed no statistical difference, PCA reveals that the differences that do appear are the rates at which those results converge. In other words, the electrical signal for nonsmokers converged to the steady-state response faster than that for smokers supported by a p-value less than 0.05 as conducted via the Wilcoxon Signed Rank test. This supports the power and sensitivity of our electrochemical sensors in that the true stimulus can be detected across varying levels of noise, but the parameters with which that detection occurs allows us to use this noise to inform us more about the category of stimulus.

Finally, we calculated statistical performance from the confusion matrix of the data in Table 1. We find a NPV of 97.6% and a specificity of 91.1%, with an overall accuracy of 89.1. In our study, we received 4 false positives and 1 false negative. Patients 5, 8, 11, and 21 were classified as positive when they were confirmed as negative by the control, while patient 2 was classified as negative when they were confirmed as positive by the control. We show the change in electrochemical response for each patient's breath against a positive response for reference in Figure S2. Our electrochemical sensors were trained to establish a positive threshold according to what the control indicated as a "positive response." In this manner, the control method of testing was considered as ground truth, and the electrochemical threshold for a positive response was constructed to attempt to maintain consistency with ground truth. Here, each bar in the chart measures nanoamperes (nA) and represents the electrochemical measurement corrected for ambient temperature, relative humidity, and pressure. Our hypothesis that the E.Co.Tech based device is robust to potential chemical interferents when screening for NO is supported by the above metrics as a result. We have summarized the materials/methods/techniques that have been used for COVID-19 sensing along with our work (Table S1).

Table 1. Confusion Matrix for the 46 Observed Subjects

	positive	negative
true	0	41
false	4	1

CONCLUSION

Electrochemistry has undiscovered potential in healthcare applications. We set out to develop a method that confirms our hypothesis that NO levels are significantly higher in the exhaled breath of COVID-19 positive patients, and that those levels are invariant to various respiratory conditions. The data acquired supports our hypothesis and the statistical methodology provides evidence that it appropriately compensates for the various factors influencing a breathomics result. Our work here gives further support for electrochemical methods to find biomarkers indicative of different respiratory conditions while remaining largely unbiased by other variables that may influence comparative methods in other works. In any clinical experiment, a patient's medical history can present many unknown confounding factors, and especially with pulmonary function experiments, a patient's smoking history is commonly known to be a differentiating factor in the results. With our work here, we demonstrate a device that is robust to a patient's current and past pulmonary conditions which helps strengthen the statistical power and overall confidence of electrochemistry as a viable technology for point-of-care diagnostics. We demonstrate our E.Co.Tech technology on a real device over 46 patients and present compelling evidence for the device's invariance to conditions such as asthma, latent tuberculosis, and the flu when analyzing a patient's fundamental respiratory response via NO detection. In future work, we intend to multiplex multiple sensors together to analyze several chemical compounds simultaneously for an even more elaborate respiratory analysis and aim to incorporate modern machine learning practices to do so. We hope our work inspires similar research in the field to emphasize the strong benefits of electrochemistry in healthcare.

MATERIALS AND METHODS

Reagents and Materials

Ionic liquid such as 1-ethyl-3-methylimidazolium tetrafluoroborate ($[EMIM]BF_4$) ≥99.0% (HPLC) was procured from MilliporeSigma. Custom-designed IDEs were procured from PCB Way. For electrochemical sensing application, we use an IDE design to develop a planar capacitive sensor using RTIL as the transducer. An IDE offers an advantage for gas sensing as it allows increased signal response due to electric field confinement. It helps in capturing the change in dielectric permittivity upon diffusion of the target gas. Moreover, gold is appropriate as the electrode material since it is electrochemically stable and possesses chemical inertness. Proper protective equipment and all safety precautions were always followed while running experiments with the toxic gas to avoid skin and eye contact or accidental inhalation and digestion of the gas.

Participants and Data

Breath sampling was performed under written consent as part of an ongoing observational study for "collection of breath samples for determination of endogenously produced VOCs and other metabolites for respiratory disease screening" regulated by the Institutional Review Board at The University of Texas at Dallas (IRB 21-442). A total of 46 subjects were recruited. Mainly 20 nonsmokers and 26 smokers were tested to study their breath profiles. Written informed consent was obtained from all participants. The study design and experimental protocols were also approved by the Institutional Review Board at The University of Texas at Dallas (IRB) number 21-442.

Table 2 indicates which subjects had underlying conditions. We report this to evaluate our technology's robustness to potentially interfering conditions. The goal of this study is to report the analytes semiquantitatively in exhaled breath of test subjects. The rationale for this study is to detect the analytes present in exhaled breath and

https://doi.org/10.1021/acsmeasuresciau.4c00020
ACS Meas. Sci. Au 2024, 4, 496−503

Table 2. Those Subjects of Whom Underlying Conditions Were Present

subject ID	underlying condition	smoker
000017	flu	no
000019	asthma	yes
000022	latent TB	yes

correlate their concentrations to the physiological state of the body. We hypothesize that there is no statistically significant difference in the electrical response between smokers and nonsmokers for this study. This can help in the development of technology that can be used as a noninvasive method for disease diagnosis using exhaled breath. The identification and recruitment of participants were done in an ethically and legally acceptable manner and were free of coercion. It should be noted that only COVID-19-negative subjects were recruited for the study. Before collecting the breath, we conducted a rapid COVID19 antigen test using commercially available test kits (iHealth COVID-19 antigen rapid test). This method shall be denoted as the control for our experiments. Once the test result was negative, the participant exhaled into the research device, and the result was represented via the accompanying custom-developed mobile application. The data obtained was deidentified and used for device performance analysis only. All the methods and study protocols on human subjects were carried out in accordance with the IRB guidelines and regulations.

Low-Cost Power Portable Microelectronic Breath Analyzer

Our original hypothesis stipulates that RTIL-based electrochemical sensors can detect a target biomarker via chronoamperometry and can do so in such a way that it is largely unbiased by other confounding factors. To validate this hypothesis, we began with a simple benchtop setup with the large electrochemical processor and a varying concentration of ambient air mixed with NO. However, in order to make this setup as practical to a real healthcare setting as possible, we developed a low-cost hand-held device with a custom circuit board and the ability to measure a single analyte, which for this application was NO. We also developed a simple iOS mobile application that could blindly receive and secure data from the device via bluetooth low-energy as each patient performed a test. The device itself performed the computation of results, but the app allowed results to be safely hidden from both the test administrator and the patient in order to preserve the blindness of the study and prevent data loss.

■ ASSOCIATED CONTENT

Data Availability Statement

All data generated or analyzed during this study are included in this published article [and its Supporting Information files].

Supporting Information

The Supporting Information is available free of charge at https://pubs.acs.org/doi/10.1021/acsmeasuresciau.4c00020.

> Confusion matrix for the data obtained using the breath analyzer device, final steady state values of the electrochemical response from each subject, temperature correction equation showing how temperature is rescaled for humidity values on the range of 10−15% (postdesiccant) and controlled for a 4.0 nA current, relative humidity correction equation showing how relative humidity is rescaled for temperature values on the range of 30−35 °C and controlled for a 4.0 nA current, table of comparison of different techniques or methods with their application (PDF)

■ AUTHOR INFORMATION

Corresponding Author

Shalini Prasad − *Department of Biomedical Engineering, University of Texas at Dallas, Richardson, Texas 75080, United States*; orcid.org/0000-0002-2404-3801; Email: shalini.prasad@utdallas.edu

Authors

Ivneet Banga − *Department of Biomedical Engineering, University of Texas at Dallas, Richardson, Texas 75080, United States*

Kordel France − *Department of Computer Science, University of Texas at Dallas, Richardson, Texas 75080, United States*

Anirban Paul − *Department of Biomedical Engineering, University of Texas at Dallas, Richardson, Texas 75080, United States*

Complete contact information is available at: https://pubs.acs.org/10.1021/acsmeasuresciau.4c00020

Author Contributions

[§]I.B. and K.F. share equal contributions. S.P., I.B., A.P., K.F. conceived the theoretical framework of the detection scheme and design of experiments. I.B., A.P. performed the sensor functionalization used in the experiments. I.B. performed the experiments. I.B., A.P., and K.F. analyzed the experimental data and drafted the paper. CRediT: **Ivneet Kaur Banga** conceptualization, data curation, formal analysis, methodology, validation, visualization, writing-original draft, writing-review & editing; **Kordel Kade France** data curation, formal analysis, methodology, validation, visualization, writing-original draft, writing-review & editing; **Anirban Paul** conceptualization, formal analysis, methodology, writing-original draft, writing-review & editing; **Shalini Prasad** conceptualization, data curation, investigation, methodology, project administration, resources, supervision, writing-original draft, writing-review & editing.

Notes

The authors declare no competing financial interest.

Statistical analyses: All the data analysis and interpretations were done using OriginPro and Python.

Ethics declarations: Dr. Shalini Prasad, Dr. Anirban Paul, Dr. Ivneet Kaur Banga and Kordel France do not have any competing interests.

■ REFERENCES

(1) Davis, H. E.; McCorkell, L.; Vogel, J. M.; Topol, E. J. Long COVID: Major Findings, Mechanisms and Recommendations. *Nat. Rev. Microbiol.* **2023**, *21* (3), 133−146.

(2) Ballering, A. V.; van Zon, S. K. R.; olde Hartman, T. C.; Rosmalen, J. G. M. Persistence of Somatic Symptoms after COVID-19 in the Netherlands: An Observational Cohort Study. *Lancet* **2022**, *400* (10350), 452−461.

(3) Bull-Otterson, L.; Baca, S.; Saydah, S. H.; Boehmer, T. K.; Adjei, S.; Gray, S.; Harris, A. M. Post−COVID Conditions Among Adult COVID-19 Survivors Aged 18−64 and ≥ 65 Years — United States, March 2020−November 2021. *Morb. Mortal. Wkly. Rep.* **2022**, *71*, 713−717.

(4) Hartung, T. J.; Neumann, C.; Bahmer, T.; Chaplinskaya-Sobol, I.; Endres, M.; Geritz, J.; Haeusler, K. G.; Heuschmann, P. U.; Hildesheim, H.; Hinz, A.; Hopff, S.; Horn, A.; Krawczak, M.; Krist, L.; Kudelka, J.; Lieb, W.; Maetzler, C.; Mehnert-Theuerkauf, A.; Montellano, F. A.; Morbach, C.; Schmidt, S.; Schreiber, S.; Steigerwald, F.; Störk, S.; Maetzler, W.; Finke, C. Fatigue and

Cognitive Impairment after COVID-19: A Prospective Multicentre Study. *eClinicalMedicine* **2022**, *53*, 101651.
(5) Adatia, A.; Wahab, M.; Shahid, I.; Moinuddin, A.; Killian, K. J.; Satia, I. Effects of Cigarette Smoke Exposure on Pulmonary Physiology, Muscle Strength and Exercise Capacity in a Retrospective Cohort with 30,000 Subjects. *PLoS One* **2021**, *16* (6), No. e0250957.
(6) Maestrelli, P.; Saetta, M.; Mapp, C. E.; Fabbri, L. M. Remodeling in Response to Infection and Injury. Airway Inflammation and Hypersecretion of Mucus in Smoking Subjects with Chronic Obstructive Pulmonary Disease. *Am. J. Respir. Crit. Care Med.* **2001**, *164*, S76−S80.
(7) Mullen, J. B.; Wright, J. L.; Wiggs, B. R.; Pare, P. D.; Hogg, J. C. Structure of Central Airways in Current Smokers and Ex-Smokers with and without Mucus Hypersecretion: Relationship to Lung Function. *Thorax* **1987**, *42* (11), 843−848.
(8) Isajevs, S.; Taivans, I.; Strazda, G.; Kopeika, U.; Bukovskis, M.; Gordjusina, V.; Kratovska, A. Decreased FOXP3 Expression in Small Airways of Smokers with COPD. *Eur. Respir. J.* **2009**, *33* (1), 61−67.
(9) Tantisuwat, A.; Thaveeratitham, P. Effects of Smoking on Chest Expansion, Lung Function, and Respiratory Muscle Strength of Youths. *J. Phys. Ther. Sci.* **2014**, *26* (2), 167−170.
(10) van Westen-Lagerweij, N. A.; Meijer, E.; Meeuwsen, E. G.; Chavannes, N. H.; Willemsen, M. C.; Croes, E. A. Are Smokers Protected against SARS-CoV-2 Infection (COVID-19)? The Origins of the Myth. *npj Prim. Care Respir. Med.* **2021**, *31* (1), 10.
(11) Korzeniowska, A.; Ręka, G.; Bilska, M.; Piecewicz-Szczęsna, H. The Smoker's Paradox during the COVID-19 Pandemic? The Influence of Smoking and Vaping on the Incidence and Course of SARS-CoV-2 Virus Infection as Well as Possibility of Using Nicotine in the Treatment of COVID-19 − Review of the Literature. *Przegl. Epidemiol.* **2021**, *75* (1), 27−44.
(12) Usman, M. S.; Siddiqi, T. J.; Khan, M. S.; Patel, U. K.; Shahid, I.; Ahmed, J.; Kalra, A.; Michos, E. D. Is There a Smoker's Paradox in COVID-19? *BMJ Evid. Based Med.* **2021**, *26* (6), 279−284.
(13) Boots, A. W.; Bos, L. D.; van der Schee, M. P.; van Schooten, F.-J.; Sterk, P. J. Exhaled Molecular Fingerprinting in Diagnosis and Monitoring: Validating Volatile Promises. *Trends Mol. Med.* **2015**, *21* (10), 633−644.
(14) Jia, Z.; Patra, A.; Kutty, V. K.; Venkatesan, T. Critical Review of Volatile Organic Compound Analysis in Breath and In Vitro Cell Culture for Detection of Lung Cancer. *Metabolites* **2019**, *9* (3), 52.
(15) Banga, I.; Paul, A.; Poudyal, D. C.; Muthukumar, S.; Prasad, S. Recent Advances in Gas Detection Methodologies with a Special Focus on Environmental Sensing and Health Monitoring Applications−A Critical Review. *ACS Sens.* **2023**, *8* (9), 3307−3319.
(16) Taylor, D. R.; Pijnenburg, M. W.; Smith, A. D.; De Jongste, J. C. Exhaled Nitric Oxide Measurements: Clinical Application and Interpretation. *Thorax* **2006**, *61* (9), 817−827.
(17) Austin, V.; Crack, P. J.; Bozinovski, S.; Miller, A. A.; Vlahos, R. COPD and Stroke: Are Systemic Inflammation and Oxidative Stress the Missing Links? *Clin. Sci.* **2016**, *130* (13), 1039−1050.
(18) Banga, I.; Paul, A.; Sardesai, A. U.; Muthukumar, S.; Prasad, S. ZEUS (ZIF-Based Electrochemical Ultrasensitive Screening) Device for Isopentane Analytics with Focus on Lung Cancer Diagnosis. *RSC Adv.* **2021**, *11* (33), 20519−20528.
(19) Banga, I.; Paul, A.; Churcher, N. K. M.; Kumar, R. M.; Muthukumar, S.; Prasad, S. Passive Breathomics for Ultrasensitive Characterization of Acute and Chronic Respiratory Diseases Using Electrochemical Transduction Mechanism. *TrAC, Trends Anal. Chem.* **2024**, *170*, 117455.
(20) Banga, I.; Paul, A.; Muthukumar, S.; Prasad, S. HELP (Hydrogen Peroxide Electrochemical Profiling): A Novel Biosensor for Measuring Hydrogen Peroxide Levels Expressed in Breath for Monitoring Airway Inflammation Using Electrochemical Methods. *Biosens. Bioelectron.: X* **2022**, *10*, 100139.
(21) Violi, F.; Oliva, A.; Cangemi, R.; Ceccarelli, G.; Pignatelli, P.; Carnevale, R.; Cammisotto, V.; Lichtner, M.; Alessandri, F.; De Angelis, M.; Miele, M. C.; D'Ettorre, G.; Ruberto, F.; Venditti, M.; Pugliese, F.; Mastroianni, C. M. Nox2 Activation in Covid-19. *Redox Biol.* **2020**, *36*, 101655.
(22) Loffredo, L.; Carnevale, R.; Cangemi, R.; Angelico, F.; Augelletti, T.; Di Santo, S.; Calabrese, C. M.; Della Volpe, L.; Pignatelli, P.; Perri, L.; Basili, S.; Violi, F. NOX2 Up-Regulation Is Associated with Artery Dysfunction in Patients with Peripheral Artery Disease. *Int. J. Cardiol.* **2013**, *165* (1), 184−192.
(23) Brooks, C. R.; Brogan, S.-B. M.; van Dalen, C. J.; Lampshire, P. K.; Crane, J.; Douwes, J. Measurement of Exhaled Nitric Oxide in a General Population Sample: A Comparison of the Medisoft HypAir FE NO and Aerocrine NIOX Analyzers. *J. Asthma* **2011**, *48* (4), 324−328.
(24) Robinson, J. K.; Bollinger, M. J.; Birks, J. W. Luminol/H2O2 Chemiluminescence Detector for the Analysis of Nitric Oxide in Exhaled Breath. *Anal. Chem.* **1999**, *71* (22), 5131−5136.
(25) Horváth, I.; Barnes, P. J.; Loukides, S.; Sterk, P. J.; Högman, M.; Olin, A.-C.; Amann, A.; Antus, B.; Baraldi, E.; Bikov, A.; Boots, A. W.; Bos, L. D.; Brinkman, P.; Bucca, C.; Carpagnano, G. E.; Corradi, M.; Cristescu, S.; de Jongste, J. C.; Dinh-Xuan, A.-T.; Dompeling, E.; Fens, N.; Fowler, S.; Hohlfeld, J. M.; Holz, O.; Jöbsis, Q.; Van De Kant, K.; Knobel, H. H.; Kostikas, K.; Lehtimäki, L.; Lundberg, J. O.; Montuschi, P.; Van Muylem, A.; Pennazza, G.; Reinhold, P.; Ricciardolo, F. L. M.; Rosias, P.; Santonico, M.; van der Schee, M. P.; van Schooten, F.-J.; Spanevello, A.; Tonia, T.; Vink, T. J. A European Respiratory Society Technical Standard: Exhaled Biomarkers in Lung Disease. *Eur. Respir. J.* **2017**, *49* (4), 1600965.
(26) Cristescu, S. M.; Mandon, J.; Harren, F. J. M.; Meriläinen, P.; Högman, M. Methods of NO Detection in Exhaled Breath. *J. Breath Res.* **2013**, *7* (1), 017104.
(27) Ibrahim, W.; Carr, L.; Cordell, R.; Wilde, M. J.; Salman, D.; Monks, P. S.; Thomas, P.; Brightling, C. E.; Siddiqui, S.; Greening, N. J. Breathomics for the Clinician: The Use of Volatile Organic Compounds in Respiratory Diseases. *Thorax* **2021**, *76* (5), 514−521.
(28) Carraro, S.; Rezzi, S.; Reniero, F.; Héberger, K.; Giordano, G.; Zanconato, S.; Guillou, C.; Baraldi, E. Metabolomics Applied to Exhaled Breath Condensate in Childhood Asthma. *Am. J. Respir. Crit. Care Med.* **2007**, *175* (10), 986−990.
(29) Banga, I.; Paul, A.; France, K.; Micklich, B.; Cardwell, B.; Micklich, C.; Prasad, S. E.Co.Tech-electrochemical handheld breath-alyzer COVID sensing technology. *Sci. Rep.* **2022**, *12* (1), 4370.
(30) Farquhar, A. K.; Henshaw, G. S.; Williams, D. E. Understanding and Correcting Unwanted Influences on the Signal from Electrochemical Gas Sensors. *ACS Sens.* **2021**, *6* (3), 1295−1304.
(31) Hitchman, M. L.; Saffell, J. R. Considerations of Thermodynamics and Kinetics for the Effects of Relative Humidity on the Electrolyte in Electrochemical Toxic Gas Sensors. *ACS Sens.* **2021**, *6* (11), 3985−3993.
(32) Karvonen, T.; Lehtimäki, L. Effect of Exhalation Flow Rates and Level of Nitric Oxide Output on Accuracy of Linear Approximation of Pulmonary Nitric Oxide Dynamics. *J. Breath Res.* **2021**, *15* (3), 036003.
(33) Hotelling, H. Analysis of a Complex of Statistical Variables into Principal Components. *J. Educ. Psychol.* **1933**, *24*, 498−520.
(34) Karl Pearson, F. R. S. LIII. On Lines and Planes of Closest Fit to Systems of Points in Space. *Philos. Mag Ser.* **1901**, *2*, 559−572.
(35) Karhunen, K.; Selin, I. *On Linear Methods in Probability Theory*; RAND Corporation: Santa Monica, CA: Santa Monica, CA, 1960.
(36) van der Maaten, L.; Hinton, G. Visualizing Data Using T-SNE. *J. Mach. Learn. Res.* **2008**, *9*, 2579−2605.

https://doi.org/10.1021/acsmeasuresciau.4c00020
ACS Meas. Sci. Au 2024, 4, 496−503